PoGaIN: Supplementary Material

Nicolas Bähler, Majed El Helou, Étienne Objois, Kaan Okumuş, and Sabine Süsstrunk, *Fellow, IEEE*.

I. Maximum Likelihood Derivation

A. Poisson-Noise Modeling

Let us denote the observed noisy image as y and the ground-truth noise-free image as x. Then, the Poisson-Gaussian model takes the form of the following equation

$$y = \frac{1}{a}\alpha + \beta, \quad \alpha \sim \mathcal{P}(ax), \quad \beta \sim \mathcal{N}(0, b^2). \tag{1}$$

Using the linearity property of expectation, we can compute the expected value

$$\mathbb{E}[y] = \frac{1}{a}\mathbb{E}[\alpha] = \frac{1}{a}ax = x. \tag{2}$$

Further, the variance has the following expression

$$\mathbb{V}[y] = \mathbb{E}\left[\left(\frac{1}{a}\alpha + \beta\right)^2\right] - x^2 = \frac{1}{a^2}\mathbb{E}[\alpha^2] + b^2 - x^2. \tag{3}$$

Given that $\mathbb{E}[\alpha^2] = ax + a^2x^2$, we have

$$\mathbb{V}[y] = \frac{x}{a} + x^2 + b^2 - x^2 = \frac{x}{a} + b^2. \tag{4}$$

B. Likelihood Function of Single-Pixel Image

From the definition of the probability mass function (PMF) of a Poisson random variable α, we get

$$\mathbb{P}[\alpha = k] = \frac{e^{-ax}(ax)^k}{k!}, \quad k \geq 0. \tag{5}$$

From the relation between the probability density function (PDF) and the PMF of discrete random variable established with the Dirac delta function, i.e. $f_X(t) = \sum_{k\in\mathbb{Z}} \mathbb{P}[X = k]\delta(t-k)$, we can derive that

$$f_\alpha(t|a,x) = \sum_{k=0}^{\infty} \frac{e^{-ax}(ax)^k}{k!}\delta(t-k). \tag{6}$$

Let us define $\alpha' = \frac{1}{a}\alpha$. Then, the cumulative distribution function (CDF) of this random variable α' has the following form

$$F_{\alpha'}(t) = \mathbb{P}[\alpha' \leq t] = \mathbb{P}[\alpha \leq at] = F_\alpha(at). \tag{7}$$

By taking the derivative of Equation (7), the PDF of α' can be found

$$f_{\alpha'}(t) = \frac{dF_{\alpha'}(t)}{dt} = \frac{dF_\alpha(at)}{dt} = af_\alpha(at). \tag{8}$$

Hence, by combining Equations (6) and (8), the likelihood function of α', which consists of the first part of the noise model, can be derived

$$\begin{aligned} f_{\alpha'}(t|a,x) &= a\sum_{k=0}^{\infty} \frac{e^{-ax}(ax)^k}{k!} \underbrace{\delta(at-k)}_{=\frac{1}{a}\delta(t-\frac{k}{a})} \\ &= \sum_{k=0}^{\infty} \frac{e^{-ax}(ax)^k}{k!}\delta(t-k/a). \end{aligned} \tag{9}$$

On the other hand, the likelihood function of a Gaussian random variable β with 0 mean is defined as

$$f_\beta(t|b) = \frac{1}{b\sqrt{2\pi}}e^{-t^2/2b^2}. \tag{10}$$

We then combine those equations and find the likelihood function of y. Since we know that α' and β are independent of each other, we have that

$$\begin{aligned} \mathcal{L}(y|a,b,x) &= (f_{\alpha'} * f_\beta)(y|a,b,x) \\ &= \sum_{k=0}^{\infty} \frac{(ax)^k}{k!b\sqrt{2\pi}} \exp\left(-ax - \frac{(y-k/a)^2}{2b^2}\right). \end{aligned} \tag{11}$$

C. Maximum Likelihood Solution for Single-Pixel Image

As derived, the maximum likelihood solution for a single-pixel image is the following

$$\begin{aligned} \hat{a}, \hat{b} &= \arg\max_{a,b} \mathcal{L}(y|a,b,x) \\ &= \arg\max_{a,b} \sum_{k=0}^{\infty} \frac{(ax)^k}{k!b\sqrt{2\pi}} \exp\left(-ax - \frac{(y-k/a)^2}{2b^2}\right). \end{aligned} \tag{12}$$

D. Likelihood Function of Multi-Pixel Image

We represent images as vectors of pixels, like y_n and x_n where $n \in \mathbb{N}$ is the index of single pixels. Hence, using this notation we obtain

$$\mathcal{L}(y_n|a,b,x_n) = \sum_{k=0}^{\infty} \frac{(ax_n)^k}{k!b\sqrt{2\pi}} \exp\left(-ax_n - \frac{(y_n-k/a)^2}{2b^2}\right). \tag{13}$$

Given x, i.e., the vector of all x_n, we can see that y_n and $y_{n'}$ are independent $\forall n \neq n'$. Therefore, we have

$$\begin{aligned} \mathcal{L}(y|a,b,x) = \prod_n \sum_{k=0}^{\infty} &\frac{(ax_n)^k}{k!b\sqrt{2\pi}} \\ &\exp\left(-ax_n - \frac{(y_n-k/a)^2}{2b^2}\right). \end{aligned} \tag{14}$$

E. Maximum Likelihood Solution for Multi-Pixel Image

Lastly, we get the following maximization problem

$$\hat{a}, \hat{b} = \arg\max_{a,b} \prod_n \sum_{k=0}^{\infty} \frac{(ax_n)^k}{k! b\sqrt{2\pi}} \exp\left(-ax_n - \frac{(y_n - k/a)^2}{2b^2}\right). \tag{15}$$

Using the strict monotonicity of the logarithm, we can simplify the optimization problem while not altering its results by using the log-likelihood $\mathcal{LL}$

$$\mathcal{LL}(y|a,b,x) = \sum_n \log\left(\sum_{k=0}^{\infty} \frac{(ax_n)^k}{k! b\sqrt{2\pi}} \exp\left(-ax_n - \frac{(y_n - k/a)^2}{2b^2}\right)\right). \tag{16}$$

Thus, the optimization problem becomes

$$\hat{a}, \hat{b} = \arg\max_{a,b} \mathcal{LL}(y|a,b,x). \tag{17}$$

In order to decrease the high computational complexity, we limit the range of k to a maximum value k_{max} which has to be chosen large enough to get a good approximation

$$\hat{a}, \hat{b} \approx \arg\max_{a,b} \sum_n \log\left(\sum_{k=0}^{k_{max}} \frac{(ax_n)^k}{k! b\sqrt{2\pi}} \exp\left(-ax_n - \frac{(y_n - k/a)^2}{2b^2}\right)\right). \tag{18}$$

With bigger values of k the log-likelihood starts to plateau and does not grow significantly anymore. Hence, by limiting the sum to a large enough k_{max}, the approximation of the log-likelihood is still good. Typically, we choose $k_{max} = 100$. We illustrate this property in the next Figure 1 where we can see how the log-likelihood is indeed reaching a plateau. We average over 25 pixels that we sample randomly, 25 linearly spaced values for $a \in [1, 100]$ and $b \in [0.01, 0.15]$. Additionally, we show the growing computation time needed to obtain those results.

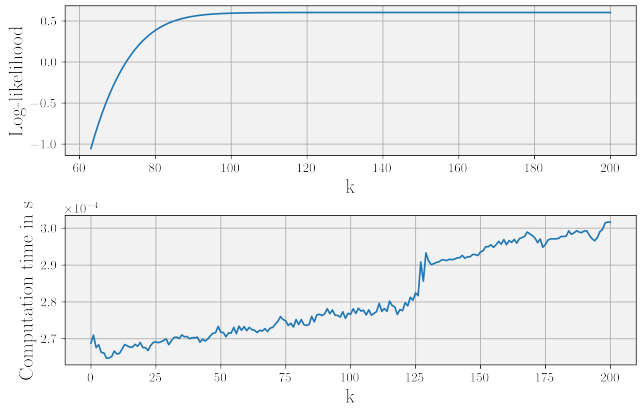

Fig. 1. The evolution of the log-likelihood with bigger k alongside the computation time.

II. Cumulants

A. The cumulant of a distribution

For a random variable X following the distribution $\mathcal{X}$, we consider the cumulant-generating function defined as

$$K_{\mathcal{X}}(t) = \log(\mathbb{E}[e^{Xt}]). \tag{19}$$

Then, we define $\kappa_r[\mathcal{X}]$, the r-th cumulant of $\mathcal{X}$, as

$$\kappa_r[\mathcal{X}] := K_{\mathcal{X}}^{(r)}(0), \tag{20}$$

with $K_{\mathcal{X}}^{(r)}(0)$ being the r-th derivative of $K_{\mathcal{X}}$ evaluated in 0.

B. Linearity

The cumulant-generating function of a sum of independent distributions is the sum of their cumulant-generating functions.

Proof.

$$\begin{aligned} K_{\mathcal{X}+\mathcal{Y}}(t) &= \log(\mathbb{E}(e^{(X+Y)t})) \\ &= \log(\mathbb{E}[e^{Xt+Yt}]) \\ &= \log(\mathbb{E}[e^{Xt}e^{Yt}]) \\ &= \log(\mathbb{E}[e^{Xt}]\mathbb{E}[e^{Yt}]) \\ &= \log(\mathbb{E}[e^{Xt}]) + \log(\mathbb{E}[e^{Yt}]) \\ &= K_{\mathcal{X}}(t) + K_{\mathcal{Y}}(t). \end{aligned} \tag{21}$$

■

C. Homogeneity

The r-th cumulant is homogeneous of degree r.

Proof.

$$\kappa_r[a\mathcal{X}] = a^r \kappa_r[\mathcal{X}]. \tag{22}$$

■

D. Unbiased estimator

For a vector x obtained by sampling independently n times from the distribution $\mathcal{X}$, the authors of **[?]** describe an unbiased estimator of $\kappa_2[\mathcal{X}], \kappa_3[\mathcal{X}]$,

$$\kappa_2[\mathcal{X}] = \frac{n}{n-1} m_2(x), \quad \kappa_3[\mathcal{X}] = \frac{n^2}{(n-1)(n-2)} m_3(x), \tag{23}$$

with m_2 being the sample variance (2-rd sample central moment) and m_3 the 3-rd sample central moment, that can be calculated using the formulae taken from **[?]**

$$\begin{aligned} m_2(x) &= \frac{n-1}{n} \sum_i (x_i - \overline{x})^2 \\ m_3(x) &= \frac{(n-1)(n-2)}{n^2} \sum_i (x_i - \overline{x})^3. \end{aligned} \tag{24}$$

E. Cumulant of Poisson-Gaussian Noise Model

We have that $\mathcal{Y} = \frac{\mathcal{P}(a\mathcal{X})}{a} + \mathcal{N}(0, b^2)$ and we want to express $\kappa_2[\mathcal{Y}]$ and $\kappa_3[\mathcal{Y}]$ as a function of a and b. First, we use Equation (21), and get that, $\kappa_r[\mathcal{Y}] = \kappa_r\left[\frac{\mathcal{P}(a\mathcal{X})}{a}\right] + \kappa_r[\mathcal{N}(0, b^2)]$.

1) Gaussian noise component: The cumulants of $\mathcal{N}(0, b^2)$ are known to be

$$\begin{aligned}\kappa_2[\mathcal{N}(0,b^2)] &= b^2\\ \kappa_3[\mathcal{N}(0,b^2)] &= 0.\end{aligned} \tag{25}$$

2) Poisson noise component: Instead of trying to find the cumulant of $\frac{\mathcal{P}(a\mathcal{X})}{a}$, we can use Equation (22), and find the cumulant of $Z \sim \mathcal{Z} = \mathcal{P}(a\mathcal{X})$

$$e^{K_{\mathcal{Z}}(t)} = \sum_k \mathbb{P}[Z=k]e^{tk}. \tag{26}$$

Moreover, we know that

$$\begin{aligned}\mathbb{P}[Z=k] &= \sum_i \mathbb{P}[X=x_i]\mathbb{P}[Z=k|X=i]\\ &= \sum_i n_i \frac{(ax_i)^k e^{-ax_i}}{k!},\end{aligned} \tag{27}$$

where $n_i = \frac{|\{\, j : x_j = x_i \,\}|}{n}$ is the proportion of intensities that are equal to a given one x_i.

Thus, we have that

$$\begin{aligned}e^{K_{\mathcal{Z}}(t)} &= \sum_k \mathbb{P}[Z=k]e^{tk}\\ &= \sum_k \sum_i n_i \frac{(ax_i)^k e^{-ax_i}}{k!}\exp(t)^k\\ &= \sum_i n_i \frac{e^{-ax_i}}{exp(-ax_i e^t)} \sum_k \frac{(ax_i e^t)^k \exp(-ax_i e^t)}{k!}\\ &= \sum_i n_i \exp(ax_i(e^t-1)).\end{aligned} \tag{28}$$

If we further note that, $f : t \mapsto \sum_i n_i \exp(ax_i(e^t-1))$, then, we get that $K_{\mathcal{Z}}(t) = \log(f(t))$. Hence, we can now compute the different derivatives of $K_{\mathcal{Z}}(t)$

$$\begin{aligned}K_{\mathcal{Z}}(t) &= \log(f(t))\\ K^1_{\mathcal{Z}}(t) &= \frac{f^{(1)}(t)}{f(t)}\\ K^2_{\mathcal{Z}}(t) &= \frac{f^{(2)}(t)f(t) - f^{(1)}(t)^2}{f(t)^2}\\ K^3_{\mathcal{Z}}(t) &= \frac{f(t)[f(t)f^{(3)}(t) - 3f^{(2)}(t)f^{(1)}(t)] + 2f^{(1)}(t)^3}{f(t)^3}.\end{aligned} \tag{29}$$

Further, by evaluating those at 0, we get

$$\begin{aligned}\kappa_0[\mathcal{Z}] &= 0\\ \kappa_1[\mathcal{Z}] &= a\overline{x}\\ \kappa_2[\mathcal{Z}] &= a\overline{x} + a^2\overline{x^2} - a^2\overline{x}^2\\ \kappa_3[\mathcal{Z}] &= a^3[\overline{x^3} - 3\overline{x^2}\,\overline{x} + 2\overline{x}^3] + a^2[3\overline{x^2} - 3\overline{x}^2] + a\overline{x},\end{aligned} \tag{30}$$

using the properties that

$$\begin{aligned}f(0) &= 1\\ f^{(1)}(0) &= a\overline{x}\\ f^{(2)}(0) &= a\overline{x} + a^2\overline{x^2}\\ f^{(3)}(0) &= a\overline{x} + 3a^2\overline{x^2} + 2a^3\overline{x^3}.\end{aligned} \tag{31}$$

Then, using Equation (22), we obtain

$$\begin{aligned}\kappa_2\left[\frac{\mathcal{P}(a\mathcal{X})}{a}\right] &= \frac{\overline{x}}{a} + \overline{x^2} - \overline{x}^2\\ \kappa_3\left[\frac{\mathcal{P}(a\mathcal{X})}{a}\right] &= \overline{x^3} - 3\overline{x^2}\,\overline{x} + 2\overline{x}^3 + 3\frac{\overline{x^2}}{a} - 3\frac{\overline{x}^2}{a} + \frac{\overline{x}}{a^2}.\end{aligned} \tag{32}$$

3) Possion-Gaussian Noise Model: By putting Equations (25) and (32) together, we obtain the complete expression of the cumulants

$$\begin{aligned}\kappa_2[\mathcal{Y}] &= \frac{\overline{x}}{a} + \overline{x^2} - \overline{x}^2 + b^2\\ \kappa_3[\mathcal{Y}] &= \overline{x^3} - 3\overline{x^2}\,\overline{x} + 2\overline{x}^3 + 3\frac{\overline{x^2}}{a} - 3\frac{\overline{x}^2}{a} + \frac{\overline{x}}{a^2}.\end{aligned} \tag{33}$$

III. CNN ARCHITECTURE

The detailed architecture of the CNN can be found in table I.

TABLE I
ARCHITECTURE OF THE CNN

Layer	Out channels	Parameters
Input	1	-
Conv2D	16	kernel_size $= (3,3)$, padding $=$ same
ReLU	16	-
BatchNorm	16	over the channels
MaxPool2D	16	pool_size $= (2,2)$
Conv2D	32	kernel_size $= (3,3)$, padding $=$ same
ReLU	32	-
BatchNorm	32	over the channels
MaxPool2D	32	pool_size $= (2,2)$
Conv2D	64	kernel_size $= (3,3)$, padding $=$ same
ReLU	64	-
BatchNorm	64	over the channels
MaxPool2D	64	pool_size $= (2,2)$
Dense	16	-
ReLU	16	-
BatchNorm	16	over the channels
Dropout	16	rate $= 0.5$
Dense	4	-
ReLU	4	-
Dense	2	-
Linear	2	-

REFERENCES

[1] Y. Zhang, Y. Zhu, E. Nichols, Q. Wang, S. Zhang, C. Smith, and S. Howard, "A Poisson-Gaussian denoising dataset with real fluorescence microscopy images," in *Proceedings of the IEEE/CVF Conference on Computer Vision and Pattern Recognition*, 2019, pp. 11 710–11 718.

[2] R. Zhou, M. El Helou, D. Sage, T. Laroche, A. Seitz, and S. Süsstrunk, "W2S: microscopy data with joint denoising and super-resolution for widefield to SIM mapping," in *European Conference on Computer Vision Workshops*, 2020, pp. 474–491.

[3] M. El Helou and S. Süsstrunk, "Blind universal Bayesian image denoising with Gaussian noise level learning," *IEEE Transactions on Image Processing*, vol. 29, pp. 4885–4897, 2020.

[4] L. D. Tran, S. M. Nguyen, and M. Arai, "GAN-based noise model for denoising real images," in *Proceedings of the Asian Conference on Computer Vision*, 2020.

[5] X. Liu, M. Tanaka, and M. Okutomi, "Single-image noise level estimation for blind denoising," *IEEE Transactions on Image Processing*, vol. 22, no. 12, pp. 5226–5237, 2013.

[6] J. Fang, S. Liu, Y. Xiao, and H. Li, "Sar image de-noising based on texture strength and weighted nuclear norm minimization," *Journal of Systems Engineering and Electronics*, vol. 27, no. 4, pp. 807–814, 2016.

[7] T. Ehret, A. Davy, J.-M. Morel, G. Facciolo, and P. Arias, "Model-blind video denoising via frame-to-frame training," in *2019 IEEE/CVF Conference on Computer Vision and Pattern Recognition (CVPR)*, 2019, pp. 11 361–11 370.

[8] S. Zhu, G. Xu, Y. Cheng, X. Han, and Z. Wang, "Bdgan: Image blind denoising using generative adversarial networks," in *Pattern Recognition and Computer Vision*, Z. Lin, L. Wang, J. Yang, G. Shi, T. Tan, N. Zheng, X. Chen, and Y. Zhang, Eds. Cham: Springer International Publishing, 2019, pp. 241–252.

[9] A. Foi, M. Trimeche, V. Katkovnik, and K. Egiazarian, "Practical Poissonian-Gaussian noise modeling and fitting for single-image raw-data," *IEEE Transactions on Image Processing*, vol. 17, no. 10, pp. 1737–1754, 2008.

[10] F. Luisier, T. Blu, and M. Unser, "Image denoising in mixed Poisson-Gaussian noise," *IEEE Transactions on Image Processing*, vol. 20, no. 3, pp. 696–708, 2011.

[11] M. Aharon, M. Elad, and A. Bruckstein, "K-SVD: An algorithm for designing overcomplete dictionaries for sparse representation," *IEEE Transactions on Signal Processing*, vol. 54, no. 11, pp. 4311–4322, 2006.

[12] S. Gu, L. Zhang, W. Zuo, and X. Feng, "Weighted nuclear norm minimization with application to image denoising," in *Computer Vision and Pattern Recognition (CVPR)*, 2014.

[13] K. Dabov, A. Foi, V. Katkovnik, and K. Egiazarian, "Image denoising by sparse 3-D transform-domain collaborative filtering," *IEEE Transactions on Image Processing*, vol. 16, no. 8, pp. 2080–2095, 2007.

[14] D. Zoran and Y. Weiss, "From learning models of natural image patches to whole image restoration," in *International Conference on Computer Vision (ICCV)*, 2011.

[15] T. Huang, S. Li, X. Jia, H. Lu, and J. Liu, "Neighbor2Neighbor: A self-supervised framework for deep image denoising," *IEEE Transactions on Image Processing*, 2022.

[16] X. Ma, X. Lin, M. El Helou, and S. Süsstrunk, "Deep Gaussian denoiser epistemic uncertainty and decoupled dual-attention fusion," in *IEEE International Conference on Image Processing (ICIP)*, 2021, pp. 1–4.

[17] K. Zhang, W. Zuo, and L. Zhang, "FFDNet: Toward a fast and flexible solution for CNN-based image denoising," *IEEE Transactions on Image Processing*, vol. 27, no. 9, pp. 4608–4622, 2018.

[18] M. El Helou and S. Süsstrunk, "BIGPrior: Towards decoupling learned prior hallucination and data fidelity in image restoration," *IEEE Transactions on Image Processing*, 2022.

[19] M. El Helou, R. Zhou, and S. Süsstrunk, "Stochastic frequency masking to improve super-resolution and denoising networks," in *European Conference on Computer Vision (ECCV)*, 2020, pp. 749–766.

[20] Q. Wang, X. Zhang, Y. Wu, L. Tang, and Z. Zha, "Nonconvex weighted ℓ_p minimization based group sparse representation framework for image denoising," *IEEE Signal Processing Letters*, vol. 24, no. 11, pp. 1686–1690, 2017.

[21] S. Cai, Z. Kang, M. Yang, X. Xiong, C. Peng, and M. Xiao, "Image denoising via improved dictionary learning with global structure and local similarity preservations," *Symmetry*, vol. 10, no. 5, p. 167, May 2018. [Online]. Available: http://dx.doi.org/10.3390/sym10050167

[22] S. Cai, K. Liu, M. Yang, J. Tang, X. Xiong, and M. Xiao, "A new development of non-local image denoising using fixed-point iteration for non-convex $_p$ sparse optimization," *PLOS ONE*, vol. 13, no. 12, pp. 1–24, 12 2018. [Online]. Available: https://doi.org/10.1371/journal.pone.0208503

[23] A. Jezierska, H. Talbot, C. Chaux, J.-C. Pesquet, and G. Engler, "Poisson-gaussian noise parameter estimation in fluorescence microscopy imaging," in *2012 9th IEEE International Symposium on Biomedical Imaging (ISBI)*, 2012, pp. 1663–1666.

[24] B. Zhang, "Contributions to fluorescence microscopy in biological imaging: PSF modeling, image restoration, and super-resolution detection," Thesis, Télécom ParisTech, Nov. 2007. [Online]. Available: https://pastel.archives-ouvertes.fr/pastel-00003273

[25] D. Martin, C. Fowlkes, D. Tal, and J. Malik, "A database of human segmented natural images and its application to evaluating segmentation algorithms and measuring ecological statistics," in *Proc. 8th Int'l Conf. Computer Vision*, vol. 2, July 2001, pp. 416–423.